

Supporting Information

Taylor et al. 10.1073/pnas.1216730109

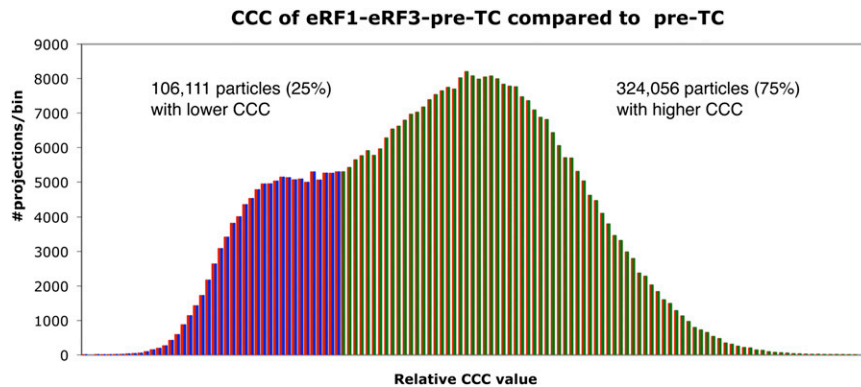


Fig. S1. Distribution of programmed vs. unprogrammed pretermination complexes (pre-TCs), as determined by cross-correlation coefficients (CCCs). Data projections for eukaryotic release factor (eRF) eRF1-eRF3-bound 80S complexes were first aligned to vacant pre-TC back projections. After alignment of images, the histogram of the CCC between the data and the reference has a bimodal appearance. Data from each mode of the histogram were used for obtaining two independent reconstructions. After angular refinement, it was evident that the images with the higher CCC (~75%) contained the density in the P site and therefore corresponded to the bona fide programmed pre-TCs. Conversely, the projections with a poorer CCC (~25%) had very weak density representing P-site tRNA and thus corresponded to nonprogrammed, vacant 80S ribosomes. These two reconstructions were used to further sort the entire dataset using supervised classification procedures (1) (Fig. S2).

1. Gao H, Valle M, Ehrenberg M, Frank J (2004) Dynamics of EF-G interaction with the ribosome explored by classification of a heterogeneous cryo-EM dataset. *J Struct Biol* 147(3): 283–290.

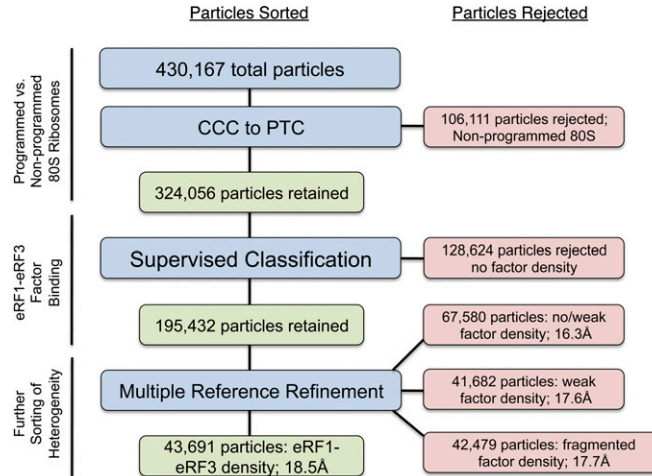


Fig. S2. Computational sorting of data projections used for the eRF1-eRF3-GMPPNP-bound 80S pre-TC. Particles totaling 430,167 were selected using semiautomated particle picking procedures (1). Of these particles, 324,056 were determined to be mRNA-bound pre-TC particles using criteria described in Fig. S1. Supervised classification algorithms (2) were used to further classify particles into two classes: those with density near the GTPase-associated center (GAC), indicative of eRF1-eRF3 binding, and those without density near the GAC. For supervised classification, we used a vacant pre-TC as the first (control) reference and the reconstructed volume with weak eRF1-eRF3 as the second reference. Supervised classification was performed iteratively to improve density levels indicative of eRF1-eRF3-bound complexes. In total, 195,432 data projections were used for further application of classification methods. Of these particles, subsets of data were determined by using different bins of data that were determined based on their cross-correlation value with the 3D reconstruction determined using all 195,432 particles. Reconstructions from particles with relatively poorer CCC resulted in 3D maps with no or very weak density corresponding to eRF1 and/or eRF3. This supervised classification was also performed iteratively, and eventually 43,691 particles were selected, which displayed the strongest density for eRF1 and eRF3 bound to the pre-TC.

1. Shaikh TR, Trujillo R, LeBarron JS, Baxter WT, Frank J (2008) Particle-verification for single-particle, reference-based reconstruction using multivariate data analysis and classification. *J Struct Biol* 164(1):41–48.
2. Gao H, Valle M, Ehrenberg M, Frank J (2004) Dynamics of EF-G interaction with the ribosome explored by classification of a heterogeneous cryo-EM dataset. *J Struct Biol* 147(3):283–290.

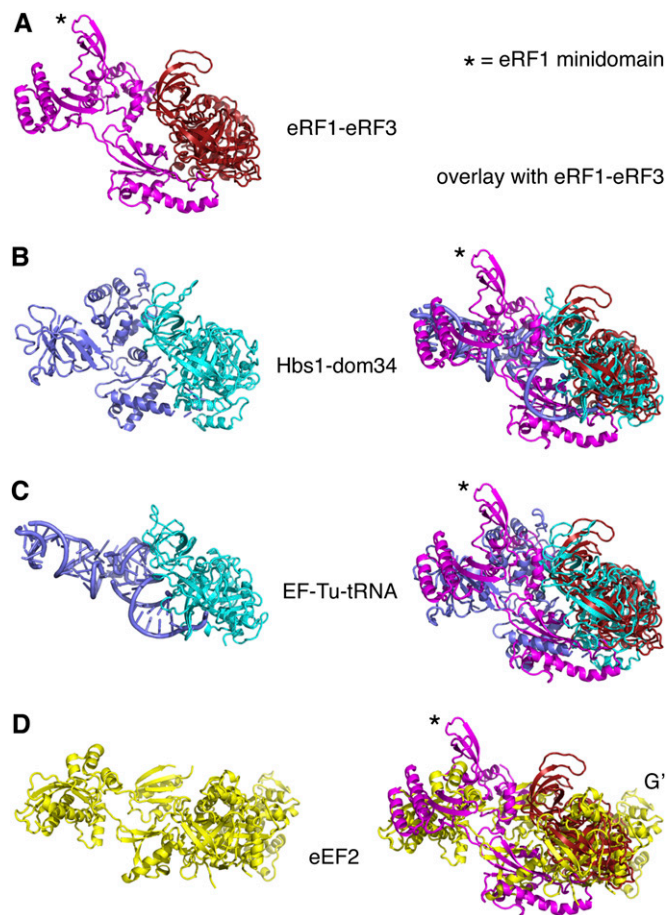


Fig. S3. Comparison of ribosomal GTPase morphologies. (A) eRF1–eRF3 from the 80S-bound cryo-EM structure. eRF1 is colored magenta and eRF3 red. The asterisk (*) identifies the unique minidomain feature of eRF1. (B) Hbs1–Dom34 from the 80S-bound ternary complex (1) alone, and overlaid with eRF1–eRF3 from the 80S-bound complex shown in A. (C) Elongation factor (EF)-Tu–tRNA from the 70S-bound complex (2) alone, and overlaid with eRF1–eRF3 from the 80S-bound complex shown in A. (D) eEF2 from the 80S-bound complex (3) alone, and overlaid with eRF1–eRF3 from the 80S-bound complex shown in A. The various overlays emphasize the point that most ribosomal GTPases have similar conformations. However, many of these factors include unique features, such as the minidomain in eRF1 and the G' domain in eEF2, which may assist in selection for their specialized functions.

1. Becker T, et al. (2011) Structure of the no-go mRNA decay complex Dom34-Hbs1 bound to a stalled 80S ribosome. *Nat Struct Mol Biol* 18(6):715–720.
2. Schmeing TM, et al. (2009) The crystal structure of the ribosome bound to EF-Tu and aminoacyl-tRNA. *Science* 326(5953):688–694.
3. Taylor DJ, et al. (2007) Structures of modified eEF2 80S ribosome complexes reveal the role of GTP hydrolysis in translocation. *EMBO J* 26(9):2421–2431.

Table S1. List of contacts between the two release factors with the ribosome

	eRF1	eRF3
40S	h14, M domain h15, M domain h32,h33,h34 in minidomain S2, NTD S3, NTD h18, NTD h30, NTD h31, NTD h34, NTD h44, NTD rpS30e, NTD rpS31e, NTD rpS31e, minidomain	h5, domain 2 h14, domain G h15, domain 2 S23, domain 2
60S	H71-AGQ in M domain H92-AGQ in M domain L23, M domain H43/44, rpL12, CTD	H95 (SRL), domain G L23, domain G L40e, domain G L9, domain 3
P-site tRNA	anticodon loop-NIKS, NTD	
eRF1 or eRF3	eRF1 (CTD)-eRF3 (domain 3) eRF1 (M domain)-eRF3 (domain G and domain 2)	

Because the map resolution is sufficient to provide accurate identification for binding interactions, a "contact" is defined as a site where the distance between the factors and the ribosome is shorter than 4 Å. CTD, C-terminal domain; NIKS, asparagine(N)-isoleucine(I)-lysine(K)-serine(S); NTD, N-terminal domain; SRL, sarcin-ricin loop.